

### Electronic Supplementary Information

Systems under study:

**1** =  $[\text{Ni}(\text{pydca})(\text{dmpy})] \cdot \text{H}_2\text{O} = \text{C}_{14}\text{H}_{14}\text{N}_2\text{NiO}_7$ , CCDC 1013574

**1b** =  $[\text{Ni}_{0.5}\text{Zn}_{0.5}(\text{pydca})(\text{dmpy})] \cdot \text{H}_2\text{O}$

pydca = pyridine-2,6-dicarboxylato

dmpy = 2,6-dimethanolpyridine, or pydm – 2,6-pyridinedimethanol.

### Synthesis and characterization of **1** and **1b**

The procedure described elsewhere has been applied.

References:

J. Miklovič, D. Valigura, R. Boča and J. Titiš, *Dalton Trans.*, 2015, 44, 12484. DOI: 10.1039/c5dt01213a

J. Miklovič, A. Packová, P. Segľa, J. Titiš, M. Koman, J. Moncol, R. Boča, V. Jorík, H. Krekuska and D. Valigura, *Inorg. Chim. Acta*, 2015, 429, 73. <http://dx.doi.org/10.1016/j.ica.2015.01.046>

For comparison:

**2** =  $[\text{Cu}(\text{pydca})(\text{dmpy})] \cdot 0.5\text{H}_2\text{O}, 2(\text{C}_{14}\text{H}_{12}\text{CuN}_2\text{O}_6), \text{H}_2\text{O} = \text{C}_{28}\text{H}_{26}\text{Cu}_2\text{N}_4\text{O}_{13}$ , CCDC 1494077

Reference: R. Boča, C. Rajnák, J. Titiš and D. Valigura, *Inorg. Chem.*, 2017, 56, 1478.

DOI: 10.1021/acs.inorgchem.6b02535

See also an analogous system:

..... $[\text{Co}(\text{dmpy})_2](\text{dnbz})_2 = \text{C}_{28}\text{H}_{24}\text{CoN}_6\text{O}_{16}$ , CCDC 1533249

$[\text{Co}_{0.41}\text{Zn}_{0.59}(\text{dmpy})_2](\text{dnbz})_2 = \text{C}_{28}\text{H}_{24}\text{Co}_{0.41}\text{N}_6\text{O}_{16}\text{Zn}_{0.59}$ , CCDC 1562425

dnbz = 3,5-dinitrobenzoato(1-).

Reference: D. Valigura, C. Rajnák, J. Moncol, J. Titiš and R. Boča, *Dalton Trans.* 2017, 46, 10950.

DOI: 10.1039/c7dt02131c

### Hardware used

For the AC susceptibility measurements the powder sample (27 mg) was encapsulated in gelatine made container and inserted into the SQUID apparatus (MPMS-XL7, Quantum Design). The AC measurement were conducted with the amplitude  $B_{\text{AC}} = 0.38$  mT. 22 frequencies between 0.1 and 1500 Hz were monitored. Ten scans have been averaged for each DC field-temperature-frequency data point. Data outside the 1 sigma-error-interval have been omitted and the rest averaged.

### Fitting the AC susceptibility data

A general formula for the complex AC susceptibility is

$$\chi(\omega) = \chi_s + \sum_{k=1}^N \frac{\chi_k - \chi_{k-1}}{1 + (i\omega\tau_k)^{1-\alpha_k}}, \quad \omega = 2\pi f, \quad \chi_0 = \chi_s$$

For the **three-set Debye model** the following relationships hold true

$$\chi(\omega) = \chi_s + \frac{\chi_{T1} - \chi_s}{1 + (i\omega\tau_1)^{1-\alpha_1}} + \frac{\chi_{T2} - \chi_{T1}}{1 + (i\omega\tau_2)^{1-\alpha_2}} + \frac{\chi_{T3} - \chi_{T2}}{1 + (i\omega\tau_3)^{1-\alpha_3}} \text{ or}$$

$$\chi(\omega) = \chi_s + (\chi_T - \chi_s) \left[ \frac{x_1}{1 + (i\omega\tau_1)^{1-\alpha_1}} + \frac{x_2}{1 + (i\omega\tau_2)^{1-\alpha_2}} + \frac{x_3}{1 + (i\omega\tau_3)^{1-\alpha_3}} \right], \quad x_3 = 1 - x_1 - x_2$$

a) the in-phase component

$$\begin{aligned} \chi'(\omega) = & \chi_s + (\chi_{T1} - \chi_s) \frac{1 + (\omega\tau_1)^{1-\alpha_1} \sin(\pi\alpha_1/2)}{1 + 2(\omega\tau_1)^{1-\alpha_1} \sin(\pi\alpha_1/2) + (\omega\tau_1)^{2-2\alpha_1}} \\ & + (\chi_{T2} - \chi_{T1}) \frac{1 + (\omega\tau_2)^{1-\alpha_2} \sin(\pi\alpha_2/2)}{1 + 2(\omega\tau_2)^{1-\alpha_2} \sin(\pi\alpha_2/2) + (\omega\tau_2)^{2-2\alpha_2}} \\ & + (\chi_{T3} - \chi_{T2}) \frac{1 + (\omega\tau_3)^{1-\alpha_3} \sin(\pi\alpha_3/2)}{1 + 2(\omega\tau_3)^{1-\alpha_3} \sin(\pi\alpha_3/2) + (\omega\tau_3)^{2-2\alpha_3}} \end{aligned}$$

b) the out-of-phase component

$$\begin{aligned} \chi''(\omega) = & (\chi_{T1} - \chi_s) \frac{(\omega\tau_1)^{1-\alpha_1} \cos(\pi\alpha_1/2)}{1 + 2(\omega\tau_1)^{1-\alpha_1} \sin(\pi\alpha_1/2) + (\omega\tau_1)^{2-2\alpha_1}} \\ & + (\chi_{T2} - \chi_{T1}) \frac{(\omega\tau_2)^{1-\alpha_2} \cos(\pi\alpha_2/2)}{1 + 2(\omega\tau_2)^{1-\alpha_2} \sin(\pi\alpha_2/2) + (\omega\tau_2)^{2-2\alpha_2}} \\ & + (\chi_{T3} - \chi_{T2}) \frac{(\omega\tau_3)^{1-\alpha_3} \cos(\pi\alpha_3/2)}{1 + 2(\omega\tau_3)^{1-\alpha_3} \sin(\pi\alpha_3/2) + (\omega\tau_3)^{2-2\alpha_3}} \end{aligned}$$

The mole fractions fulfil

$$\begin{aligned} (\chi_{T1} - \chi_s) &= (\chi_T - \chi_s)x_1, \quad (\chi_{T2} - \chi_{T1}) = (\chi_T - \chi_s)x_2, \quad (\chi_{T3} - \chi_{T2}) = (\chi_T - \chi_s)x_3, \quad \chi_{T3} = \chi_T \\ x_1 &= (\chi_{T1} - \chi_s)/(\chi_T - \chi_s), \quad x_2 = (\chi_{T2} - \chi_{T1})/(\chi_T - \chi_s), \quad x_3 = (\chi_{T3} - \chi_{T2})/(\chi_T - \chi_s) \end{aligned}$$

Ten free parameters ( $\chi_s$ ,  $\chi_{T1}$ ,  $\chi_{T2}$ ,  $\chi_{T3}$ ,  $\alpha_1$ ,  $\alpha_2$ ,  $\alpha_3$ ,  $\tau_1$ ,  $\tau_2$ , and  $\tau_3$ ) can be fitted reliably by using 44 experimental data points. The functional to be minimized accounts to the relative errors of both susceptibility components

- $F = w \cdot E(\chi') + (1-w) \cdot E(\chi'')$  with the typical weight  $w = 0.07$ , or
- $F = E(\chi') \cdot E(\chi'')$  with

$$E(\chi) = (1/N) \left[ \sum_i^N \left| (\chi_i^e - \chi_i^c) / \chi_i^c \right| \right]$$

The optimization routine refers to the genetic algorithm of D. L. Carroll, Univ. Illinois, Urbana, USA, 1998.  
 The quality of the fit is expressed by

- a) **discrepancy factors** for the in-phase and out-of phase susceptibilities  $R(\chi')$  and  $R(\chi'')$  defined as

$$R(\chi) = \sqrt{\left[ \sum_i (\chi_i^e - \chi_i^c)^2 \right] / \left[ \sum_i (\chi_i^c)^2 \right]}$$

- b) **by the standard deviation** for each optimized parameter; this is given in parentheses, e.g. 12.7(25) means  $12.7 \pm 2.5$  (at 95% probability level).

The retrieved parameters should follow a systematic trend along a smooth dependence.

The **two-set Debye model** follows from the truncation of the three-set model.

**Field dependence of the slow magnetic relaxation for **1****

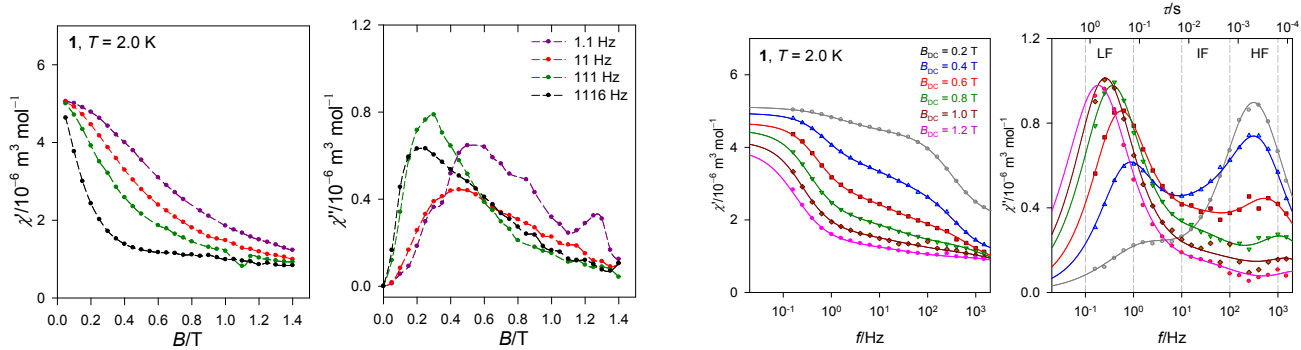


**Figure S1** Field/frequency dependence of the AC susceptibility components for **1** at  $T = 2.0\text{ K}$ .

**Table S1.** Results of the fitting procedure for AC susceptibility components of **1** at  $T = 2.0\text{ K}$  using three-set Debye model

$B_{DC}$ $/\text{T}$	$R(\chi')$ $/\%$	$R(\chi'')$ $/\%$	$\chi_S$	$\chi_{LF}$	$\alpha_{LF}$	$\tau_{LF}$ $/10^{-3}\text{ s}$	$\chi_{IF}$	$\alpha_{IF}$	$\tau_{IF}$ $/10^{-3}\text{ s}$	$\chi_{HF}$	$\alpha_{HF}$	$\tau_{HF}$ $/10^{-6}\text{ s}$	$x_{LF}$	$x_{IF}$	$x_{HF}$
0.2	0.18	1.8	2.00(1)	2.69(3)	0.32(2)	100(5)	-	-	-	5.12(1)	0.20(1)	496(5)	0.22	-	0.78
0.4	0.41	1.4	1.01(10)	2.2(6)	0.12(8)	222(15)	3.5(11)	0.43(37)	6.6(67)	4.95(6)	0.16(11)	403(44)	0.30	0.33	0.37
0.6	0.68	3.0	0.67(44)	2.2(9)	0.07(8)	322(16)	4.3(9)	0.60(28)	6.2	4.8(3)	0.07	201(42)	0.38	0.50	0.12
0.8	0.82	2.4	0.78(9)	3.2(1)	0.16(2)	456(14)	4.0(2)	0.35(12)	6.2(15)	4.5(1)	0.10(18)	120	0.65	0.22	0.13
1.0	2.4	5.7	0.78(24)	3.2(6)	0.14(7)	636(46)	4.0(7)	0.51(50)	5.0(65)	4.2(1)	0.00	86	0.71	0.23	0.06
1.2	1.7	4.0	0.78(32)	3.4(3)	0.20(4)	876(65)	3.8(4)	0.35(24)	5.0(25)	4.0(1)	0.00	60	0.81	0.13	0.06

Mole fractions:  $x_{LF} = (\chi_T,LF - \chi_S)/(\chi_T - \chi_S)$ ,  $x_{IF} = (\chi_T,IF - \chi_{T,LF})/(\chi_T - \chi_S)$ ,  $x_{HF} = (\chi_{T,HF} - \chi_{T,IF})/(\chi_T - \chi_S)$ ,  $\chi_{T,HF} = \chi_T$ , and  $x_{IF} = 1 - x_{LF} - x_{HF}$ . SI unit for the molar magnetic susceptibility [ $10^{-6}\text{ m}^3\text{ mol}^{-1}$ ]. Standard deviations in parentheses (last digit).  $R$  – discrepancy factor of the fit for dispersion  $\chi'$  and absorption  $\chi''$ , respectively.

Note: the AC-susceptibility response is rather scattered in the stronger magnetic fields due to low amplitude  $B_{AC} = 0.38\text{ mT}$  (hardware limit) and lower stability of the DC field  $B_{DC}$ .

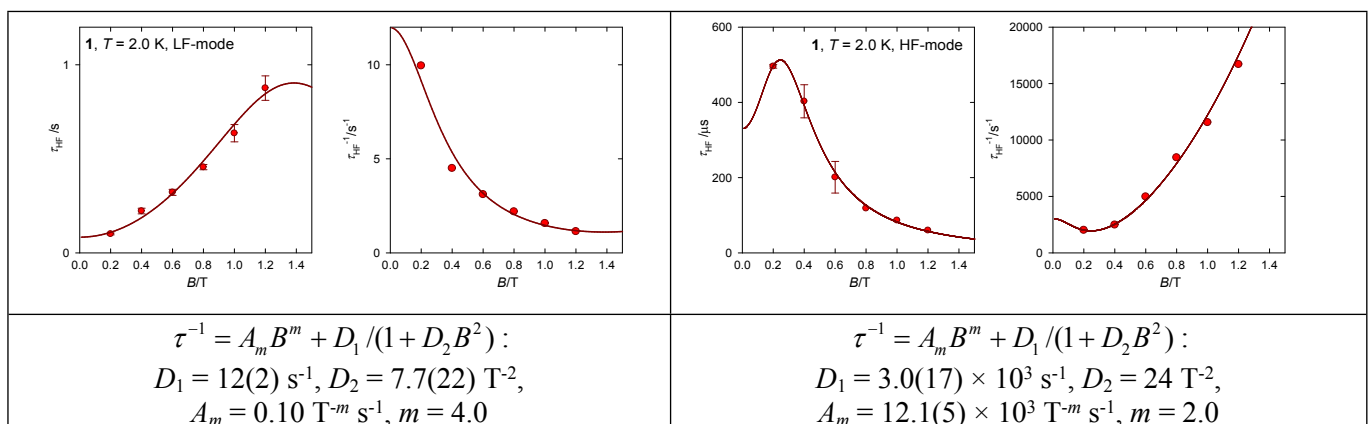


**Figure S2** Field dependence of the relaxation time for **1**. Solid lines – fitted.

Temperature dependence of the AC susceptibility components for **1**

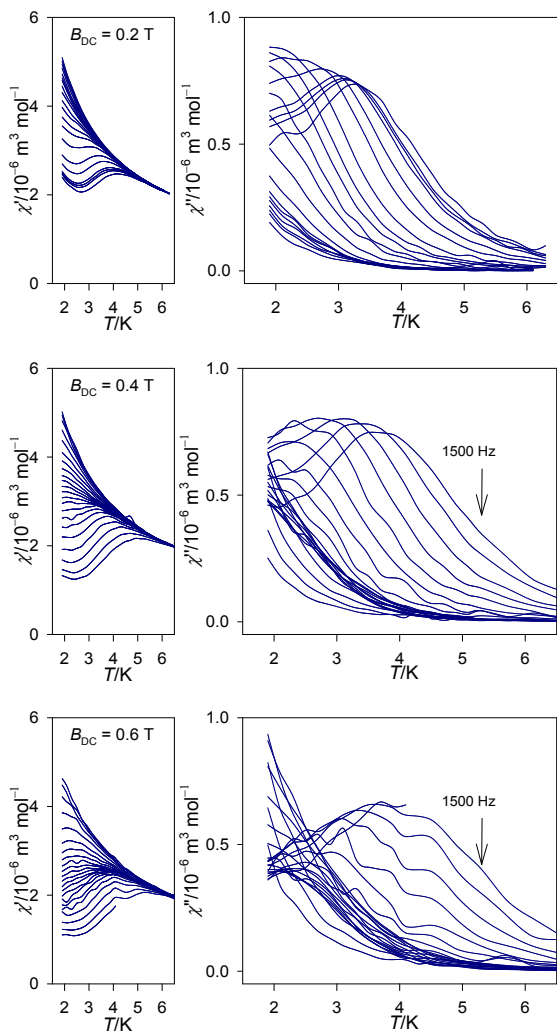
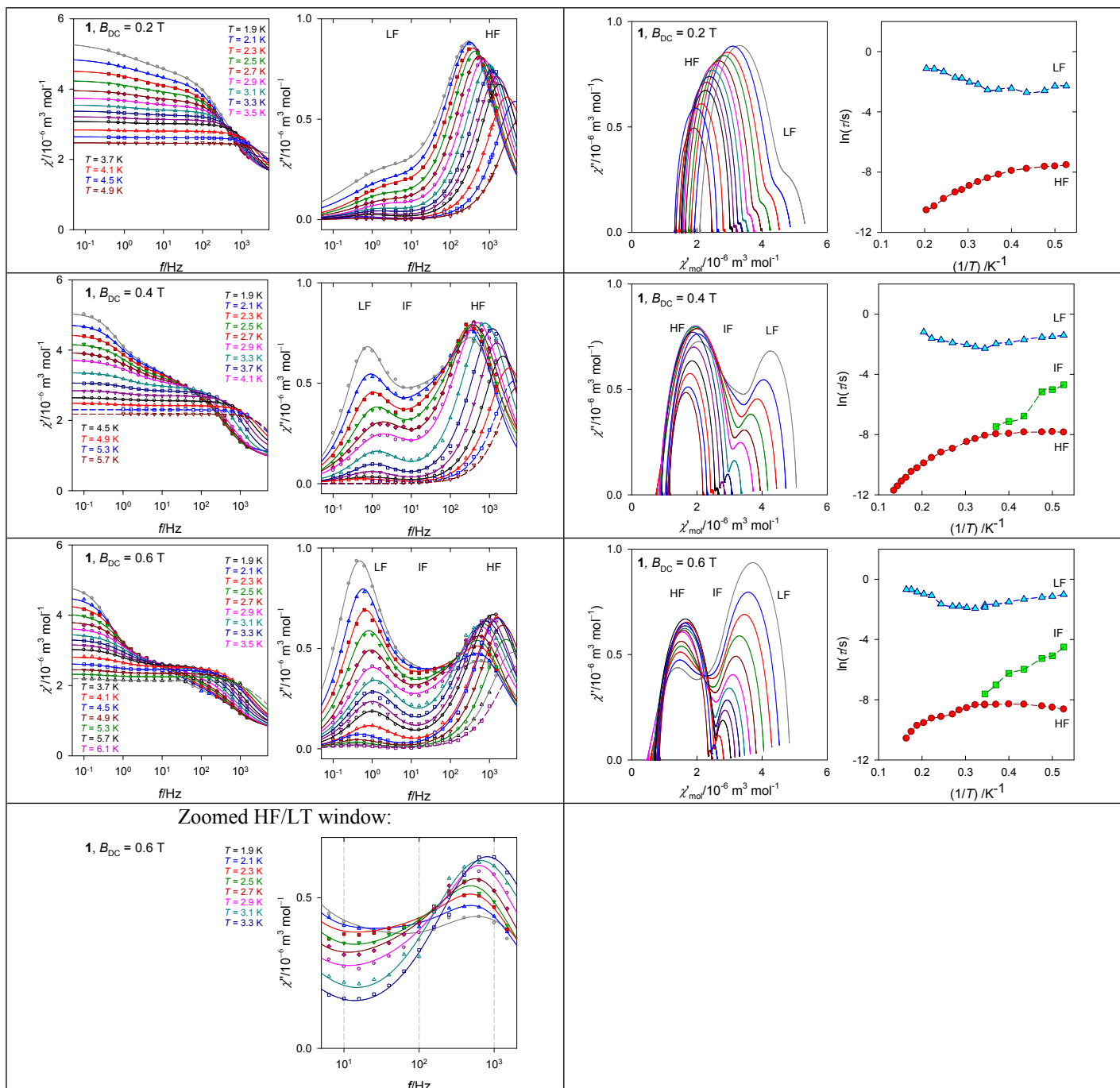


**Figure S3** Temperature dependence of the AC susceptibility components for **1** at the external magnetic field for a set of frequencies ranging between  $f = 0.1$  and 1500 Hz.



#### Doping experiments

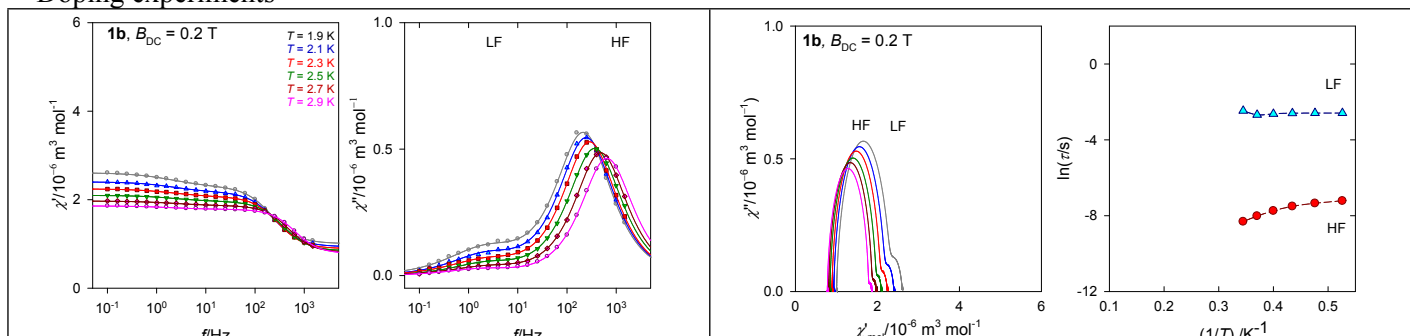


**Figure S4** Comparison of AC susceptibility components for **1** and **1b** at different external fields. Intermediate-frequency mode merges with the high-frequency one after some temperature threshold.

**Table S2.** Results of the fitting procedure for AC susceptibility components of **1** using a three-set (two-set) Debye model

a)  $B_{DC} = 0.2$  T

T/K	$R(\chi')/\%$	$R(\chi'')/\%$	$\chi_s$	$\chi_{T1}$	$\alpha_1$	$\tau_1 / 10^{-3}$ s	$\chi_{T2}$	$\alpha_2$	$\tau_2 / 10^{-6}$ s	$x_{LF}$	$x_{HF}$
1.9	0.13	1.1	2.08(1)	3.17(8)	0.51(3)	<b>102(8)</b>	5.44(4)	0.19(1)	538(5)	0.32	0.68
2.0	0.18	1.8	2.00(1)	2.69(3)	0.32(2)	<b>100(5)</b>	5.12(1)	0.20(1)	496(5)	0.22	0.78
2.1	0.34	1.1	1.92(1)	2.63(9)	0.44(6)	<b>75(10)</b>	4.89(4)	0.18(1)	483(7)	0.24	0.76
2.3	0.35	1.0	1.81(1)	2.33(6)	0.36(5)	<b>66(7)</b>	4.53(2)	0.17(1)	423(5)	0.19	0.81
2.5	0.51	0.94	1.75(2)	2.13(6)	0.33(8)	<b>86(16)</b>	4.25(3)	0.15(1)	367(5)	0.15	0.85
2.7	0.34	0.52	1.64(1)	1.93(4)	0.34(7)	<b>81(12)</b>	3.97(2)	0.15(1)	286(3)	0.12	0.88
2.9	0.29	0.72	1.58(1)	1.80(3)	0.30(6)	<b>78(11)</b>	3.74(1)	0.13(1)	225(2)	0.10	0.90
3.1	0.32	1.1	1.55(2)	1.70(4)	0.28(10)	<b>113(27)</b>	3.55(2)	0.12(1)	175(2)	0.08	0.92
3.3	0.17	1.0	1.52(1)	1.64(2)	0.28(7)	<b>131(26)</b>	3.38(1)	0.10(1)	136(2)	0.07	0.93
3.5	0.28	1.6	1.46(3)	1.54(4)	0.17(15)	<b>170(61)</b>	3.21(2)	0.10(1)	103(3)	0.04	0.96
3.7	0.27	0.70	1.51(3)	1.57(3)	0.17(16)	<b>178(67)</b>	3.08(1)	0.07(1)	88(2)	0.04	0.96
4.1	0.26	1.3	1.45(5)	1.49(6)	0.07(30)	<b>262(181)</b>	2.84(2)	0.07(1)	57(3)	0.02	0.98
4.5	0.17	2.2	1.32(8)	1.34(8)	0.02(24)	<b>316(176)</b>	2.64(1)	0.06(1)	35(3)	0.02	0.98
4.9	0.24	3.1	1.36(16)	1.37(16)	0.00	<b>325</b>	2.47(1)	0.07(2)	27(5)	0.01	0.99

b)  $B_{DC} = 0.4$  T

T/K	$R(\chi')/\%$	$R(\chi'')/\%$	$\chi_s$	$\chi_{LF}$	$\alpha_{LF}$	$\tau_{LF} / 10^{-3}$ s	$\chi_{IF}$	$\alpha_{IF}$	$\tau_{IF} / 10^{-3}$ s	$\chi_{HF}$	$\alpha_{HF}$	$\tau_{HF} / 10^{-6}$ s	$x_{LF}$	$x_{IF}$	$x_{HF}$
1.9	0.39	1.7	1.02(3)	2.3(2)	0.06(4)	<b>245(12)</b>	3.5(4)	0.37(17)	9.2(26)	5.06(2)	0.18(5)	391(39)	0.32	0.30	0.39
2.0	0.41	1.4	1.01(10)	2.2(6)	0.12(8)	<b>222(15)</b>	3.5(11)	0.43(37)	6.6(67)	4.94(5)	0.16(11)	403(44)	0.30	0.33	0.37
2.1	0.49	1.7	1.05(3)	2.1(3)	0.11(5)	<b>213(18)</b>	3.3(6)	0.36(22)	5.7(33)	4.73(2)	0.11(7)	395(39)	0.29	0.33	0.39
2.3	0.60	2.4	0.84(13)	1.7(2)	0.12(5)	<b>182(12)</b>	3.6(6)	0.47(6)	1.11(8)	4.46(2)	0.02(14)	393(37)	0.24	0.52	0.24
2.5	0.38	1.7	0.85(8)	1.7(1)	0.16(3)	<b>150(8)</b>	3.4(5)	0.42(5)	0.80(41)	4.18(1)	0.01(12)	358(25)	0.26	0.51	0.23
2.7	0.24	1.6	0.80(6)	1.45(9)	0.17(3)	<b>139(8)</b>	3.0(5)	0.44(8)	0.56(22)	3.93(1)	0.04(9)	348(18)	0.21	0.50	0.29
2.9	0.21	2.2	0.84(2)	1.54(3)	0.27(2)	<b>102(4)</b>	-	-	-	3.73(1)	0.20(1)	313(4)	0.24	-	0.76*
3.1	0.27	1.8	0.86(2)	1.39(3)	0.24(2)	<b>114(5)</b>	-	-	-	3.54(1)	0.19(1)	253(3)	0.20	0.80	
3.3	0.29	2.1	0.89(2)	1.29(3)	0.16(2)	<b>130(6)</b>	-	-	-	3.36(1)	0.16(1)	207(3)	0.16	0.84	
3.7	0.29	2.7	0.91(3)	1.14(4)	0.13(4)	<b>149(10)</b>	-	-	-	3.07(1)	0.14(1)	131(3)	0.11	0.89	
4.1	0.37	2.8	1.11(4)	1.26(4)	0.17(6)	<b>178(21)</b>	-	-	-	2.84(1)	0.08(1)	103(4)	0.09	0.91	
4.5	0.39	1.8	1.15(5)	1.25(5)	0.25(9)	<b>200(43)</b>	-	-	-	2.65(1)	0.07(1)	72(4)	0.07	0.93	
4.9	0.27	2.9	1.15	1.22(1)	0.26(9)	<b>302(74)</b>	-	-	-	2.49(1)	0.06(1)	50(1)	0.05	0.95	
5.3	0.38	7.2	1.15	-	-	-	-	-	-	2.30(1)	0.08(1)	36.3(10)	-	-	1
5.7	0.35	7.5	1.15	-	-	-	-	-	-	2.18(1)	0.04(1)	28.5(9)	-	-	
6.13	0.35	1.2	1.15	-	-	-	-	-	-	2.07(1)	0.08(2)	19.2(11)	-	-	
6.55	0.30	8.1	1.15	-	-	-	-	-	-	1.97(1)	0.07(2)	15.0(9)	-	-	
6.97	0.55	32	1.15	-	-	-	-	-	-	1.88(3)	0.07(6)	10.8(22)	-	-	
7.39	0.46	24	1.1	-	-	-	-	-	-	1.81(1)	0.08(6)	8.2(18)	-	-	

\* Above  $T > 2.7$  K the IF mode merges with HF and then the mole fractions merge to  $x_{HF}$  only.

c)  $B_{DC} = 0.6$  T

T/K	$R(\chi')/\%$	$R(\chi'')/\%$	$\chi_s$	$\chi_{LF}$	$\alpha_{LF}$	$\tau_{LF} / 10^{-3}$ s	$\chi_{IF}$	$\alpha_{IF}$	$\tau_{IF} / 10^{-3}$ s	$\chi_{HF}$	$\alpha_{HF}$	$\tau_{HF} / 10^{-6}$ s	$x_{LF}$	$x_{IF}$	$x_{HF}$
1.9	0.78	2.7	0.78(9)	2.7(5)	0.12(5)	<b>367(14)</b>	4.2(6)	0.48(25)	7.0	4.90(7)	0.12(18)	200(23)	0.48	0.35	0.18
2.0	0.66	3.0	0.72(36)	2.3(10)	0.08(9)	<b>327(16)</b>	4.2(11)	0.58(33)	7.7	4.77(22)	0.10(26)	211(34)	0.39	0.47	0.14
2.1	1.1	2.0	0.69(29)	2.1(9)	0.06(9)	<b>305(15)</b>	3.9(10)	0.56(29)	6.2	4.58(2)	0.14(26)	220(35)	0.36	0.47	0.18
2.3	0.88	2.9	0.71(37)	2.0(9)	0.08(9)	<b>265(12)</b>	3.5(15)	0.52(48)	3.7	4.32(13)	0.13(35)	237(32)	0.36	0.43	0.21
2.5	0.72	2.6	0.69(43)	1.9(6)	0.12(5)	<b>220(10)</b>	3.4(12)	0.52(24)	4.0	4.07(6)	0.10(32)	250(53)	0.35	0.44	0.21
2.7	0.63	2.9	0.67(21)	1.4(4)	0.07(8)	<b>210(14)</b>	3.0(6)	0.59(12)	4.6	3.91(10)	0.12(12)	256(19)	0.23	0.49	0.28
2.9	0.659	3.6	0.67(35)	1.3(4)	0.06(8)	<b>191(11)</b>	2.8(6)	0.50(13)	2.0	3.67(7)	0.06(140)	250(26)	0.22	0.49	0.29
2.9	0.85	3.6	0.48(7)	1.5(1)	0.22(3)	<b>150(7)</b>	-	-	-	3.65(2)	0.35(2)	249(18)	0.34	-	0.66
3.1	0.74	4.9	0.62(6)	1.5(1)	0.19(3)	<b>144(7)</b>	-	-	-	3.47(2)	0.28(2)	232(14)	0.31	0.69	
3.3	0.32	4.1	0.71(4)	1.44(5)	0.18(1)	<b>152(6)</b>	-	-	-	3.32(1)	0.25(1)	200(7)	0.28	0.72	
3.5	0.29	4.0	0.76(3)	1.36(4)	0.17(2)	<b>166(6)</b>	-	-	-	3.17(1)	0.21(1)	168(6)	0.25	0.75	
3.7	0.30	1.6	0.71(3)	1.16(3)	0.15(2)	<b>165(5)</b>	-	-	-	3.03(1)	0.21(1)	128(3)	0.19	0.81	
4.1	1.1	4.2	0.87(10)	1.16(11)	0.15(8)	<b>194(30)</b>	-	-	-	2.80(2)	0.15(3)	108(11)	0.15	0.85	
4.5	0.51	3.4	0.80(9)	0.97(9)	0.10(7)	<b>338(41)</b>	-	-	-	2.62(1)	0.15(2)	97(9)	0.09	0.91	
4.9	0.29	2.5	0.84(9)	0.95(10)	0.14(7)	<b>374(55)</b>	-	-	-	2.45(1)	0.13(2)	72(7)	0.07	0.93	
5.3	0.69	3.4	0.96(20)	1.04(20)	0.10(17)	<b>427(139)</b>	-	-	-	2.32(1)	0.11(3)	60(14)	0.05	0.95	
5.7	0.83	11	0.96	1.01(2)	0.12(31)	<b>500(329)</b>	-	-	-	2.20(2)	0.13(3)	40(3)	0.04	0.96	
6.1	0.56	6.6	0.96	0.99(1)	0.07(26)	<b>505(241)</b>	-	-	-	2.09(1)	0.17(2)	26(2)	0.03	0.97	

Above  $T > 2.9$  K the IF mode merges with HF and then the mole fractions merge to  $x_{HF}$  only.

d) Doping experiment: **1b**,  $w_{Ni} = 0.5$ ; Ni:Zn = 1:1,  $B_{DC} = 0.2$  T

T/K	$R(\chi')/\%$	$R(\chi'')/\%$	$\chi_s$	$\chi_{T1}$	$\alpha_1$	$\tau_1 / 10^{-3}$ s	$\chi_{T2}$	$\alpha_2$	$\tau_2 / 10^{-6}$ s	$x_{LF}$	$x_{HF}$
1.9	0.32	1.8	1.00(1)	1.33(1)	0.28(3)	<b>75(5)</b>	2.61(1)	0.09(1)	733(7)	0.20	0.80
2.1	0.28	1.7	0.93(1)	1.17(1)	0.24(3)	<b>75(5)</b>	2.40(1)	0.09(1)	643(5)	0.16	0.84
2.3	0.25	1.6	0.89(1)	1.07(1)	0.27(3)	<b>74(6)</b>	2.24(1)	0.07(1)	548(4)	0.13	0.87
2.5	0.31	1.2	0.84(1)	0.97(1)	0.23(4)	<b>72(6)</b>	2.10(1)	0.07(1)	433(3)	0.11	0.89
2.7	0.22	1.2	0.81(1)	0.91(1)	0.28(4)	<b>68(7)</b>	1.97(1)	0.05(1)	328(2)	0.09	0.91
2.9	0.18	0.71	0.78(1)	0.85(1)	0.24(4)	<b>85(7)</b>	1.86(1)	0.05(1)	245(2)	0.07	0.93

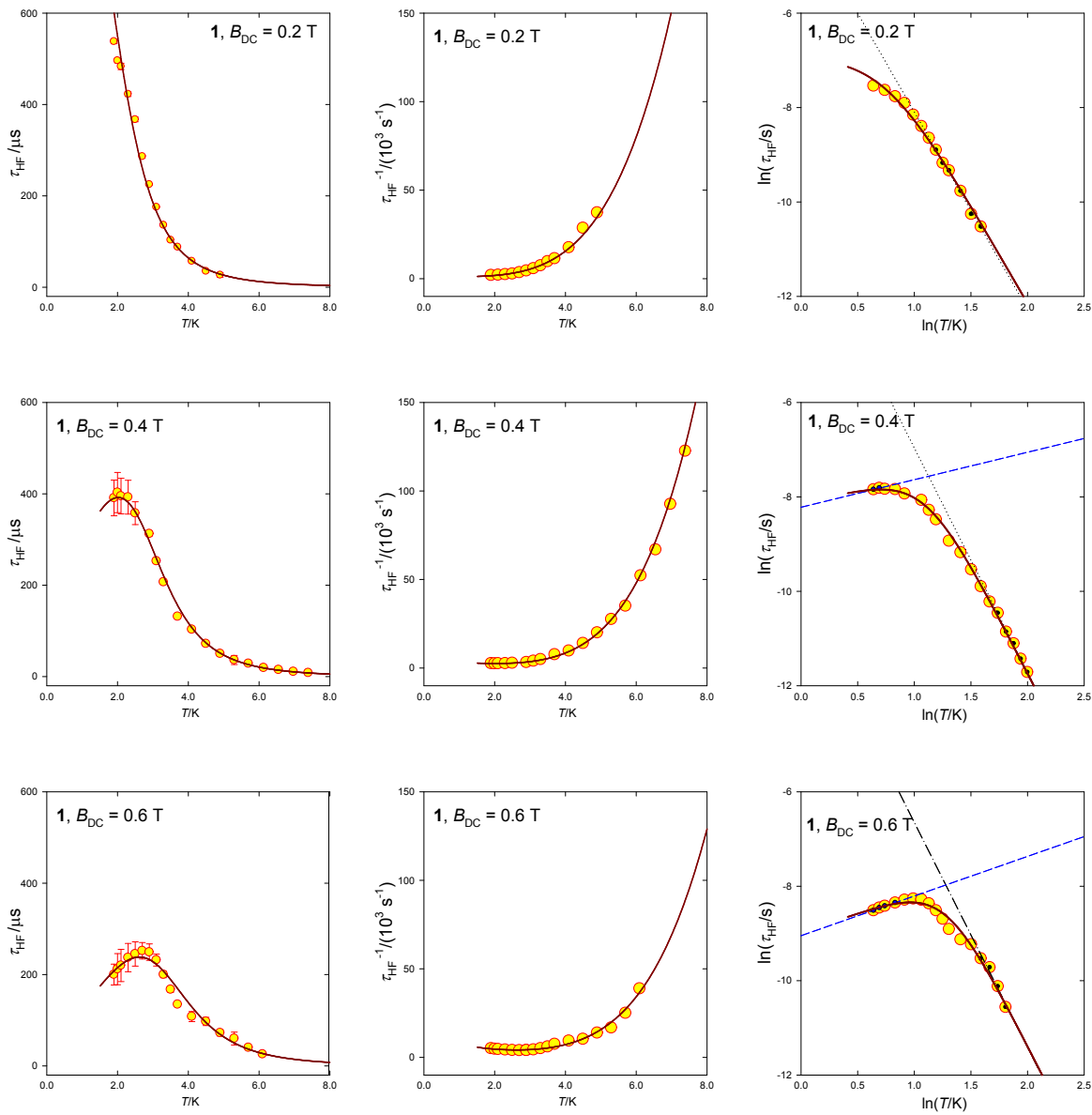


**Figure S5** Plot of the relaxation rates for HF relaxation channel of **1**. Solid lines – fitted with the truncated relaxation equation  $\tau^{-1} = CT^n + E_1 T^{-k}$ . Straight lines – linear dependence in the intermediate temperature region (Raman term) and the lowest temperature region (“strange term”); full points – selection for the linear fit. Error bars for the fit are also displayed.

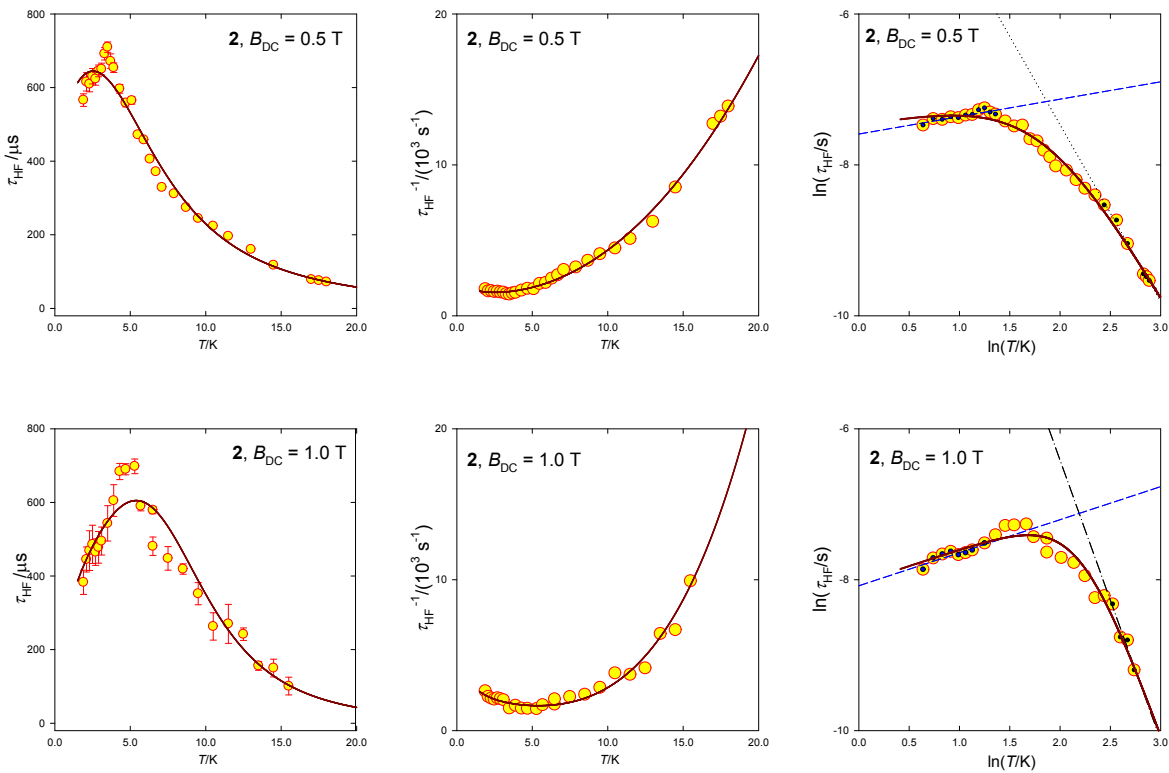


**Figure S6** For comparison: plot of the relaxation rates for HF relaxation channel of **2**. Solid lines – fitted with the truncated relaxation equation  $\tau^{-1} = CT^n + E_1 T^{-k}$ . Straight lines – linear dependence in the intermediate temperature region (Raman term) and the lowest temperature region (“strange term”); full points – selection for the linear fit.

**Table S4** Parameters of the relaxation process for the high-frequency channel of **1** and **2**<sup>a</sup>

	<b>1</b>	<b>1</b>	<b>1</b>	<b>2</b>	<b>2</b>
Parameter	$B_{DC} = 0.2 \text{ T}$	$B_{DC} = 0.4 \text{ T}$	$B_{DC} = 0.6 \text{ T}$	$B_{DC} = 0.5 \text{ T}$	$B_{DC} = 1.0 \text{ T}$
<i>Net Raman process in the intermediate temperature region</i>					
$n$	4.17	4.7	4.76	2.3	3.7
$C / \text{T}^{-n} \text{ s}^{-1}$	50	9.1	6.6	16	0.36
<i>Net “strange” process in the lowest temperature region</i>					
$k$	-	0.58	0.84	0.23	0.44
$E_1 / \text{T}^k \text{ s}^{-1}$	-	$3.7 \times 10^3$	$8.51 \times 10^3$	1978	3231
<i>Whole temperature region</i>					
$n$	[4.17]	[4.7]	[4.76]	[2.3]	[3.7]
$C / \text{T}^{-n} \text{ s}^{-1}$	50.0(17)	10.3(2)	6.4(3)	16.7(5)	0.34(2)
$k$	-	[0.58]	[0.84]	[0.23]	[0.44]
$E_1 / \text{T}^k \text{ s}^{-1}$	-	$3.4(1) \times 10^3$	$8.0(3) \times 10^3$	$1.7(1) \times 10^3$	$3.1(1) \times 10^3$
$D_1 / \text{s}^{-1}$	1008(104)	[0]	[0]	[0]	[0]

<sup>a</sup> General relaxation equation  $\tau^{-1} = \tau_0^{-1} \exp(-U / k_B T) + CT^n + AB^m T + D_1 / (D_2 + B^2) + E_1 T^{-k}$

The data fitting in the whole temperature region was preceded by linear fits:

- a)  $\ln \tau = -\ln C - n \ln T$  in the intermediate temperature region,
- b)  $\ln \tau = -\ln E_1 + k \ln T$  in the lowest temperature region.

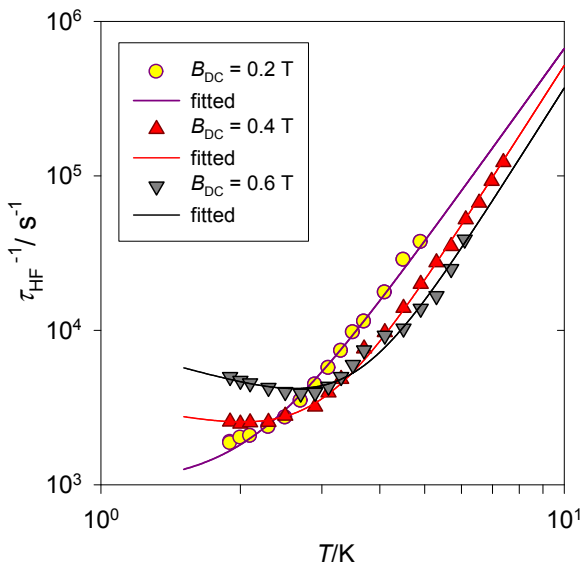


**Figure S7** Comparison of the relaxation time for **1** at different external fields.

#### Doping experiments

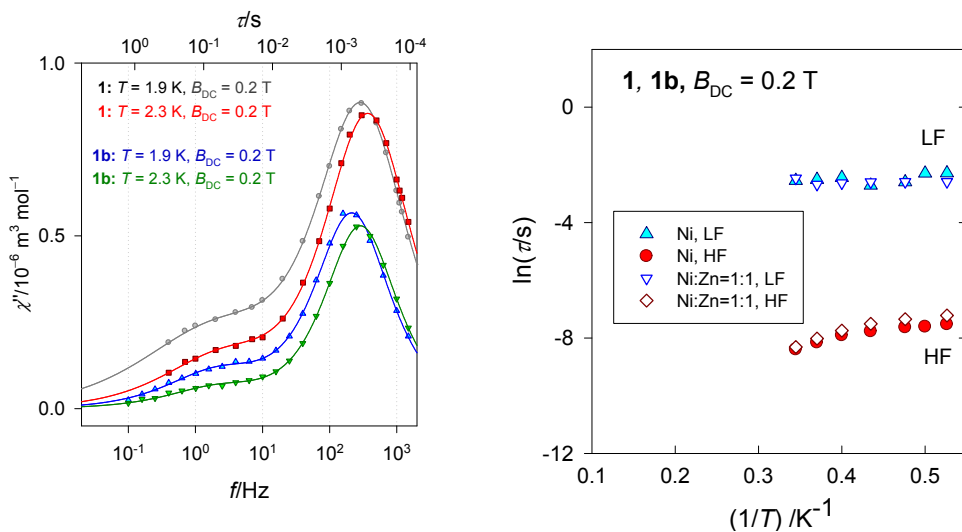


**Figure S8.** Comparison of AC susceptibility data for **1** and **1b** at  $B_{DC} = 0.2\text{ T}$ .

There is a slight increase of the HF-mole fraction  $x_{HF}$  for **1b** relative to **1**. Relaxation time of the HF mode  $\tau_{HF}$  is higher for **1b** relative to **1** (on dilution the Ni-system is relaxing more slowly).

### Modelling of the two-set susceptibility

According to [L. T. A. Ho and L. Chibotaru, Phys. Rev. 2016, B94, 104422] a three-level model offers the susceptibility expressions (in their original symbolism)

$$\chi'(\omega) = \frac{1}{T} \frac{c}{1+2c} \left( m_{11}^2 \frac{1}{1+\omega^2\tau_2^2} + \frac{m_{33}^2}{1+2c} \frac{1}{1+\omega^2\tau_3^2} \right)$$

$$\chi''(\omega) = \frac{1}{T} \frac{c}{1+2c} \left( m_{11}^2 \frac{\omega\tau_2}{1+\omega^2\tau_2^2} + \frac{m_{33}^2}{1+2c} \frac{\omega\tau_3}{1+\omega^2\tau_3^2} \right)$$

The relaxation rates involving the direct and Orbach terms are

$$\text{HF mode: } \lambda_2 / \Gamma_0 = aT + \Gamma_0 / (c-1) = A(\Delta / kT) + 1 / (c-1), \quad \tau_2^{-1} = \lambda_2$$

$$\text{LF mode: } \lambda_3 / \Gamma_0 = (2c+1) / (c-1), \quad \tau_3^{-1} = \lambda_3$$

with  $A = a(\Delta / k) / \Gamma_0$  and  $c = \exp(\Delta / kT)$ ;  $\omega = 2\pi f$ .

(Notice, the direct term is field-dependent  $\lambda_{\text{direct}} = A_{\text{direct}} B^n T = a_n T$  with typical values of  $n = 2 - 4$ .)

Using  $m_{11} = m_{33} = 1$ , the AC susceptibility components and the Argand (Cole-Cole) diagram have been modelled as follows.

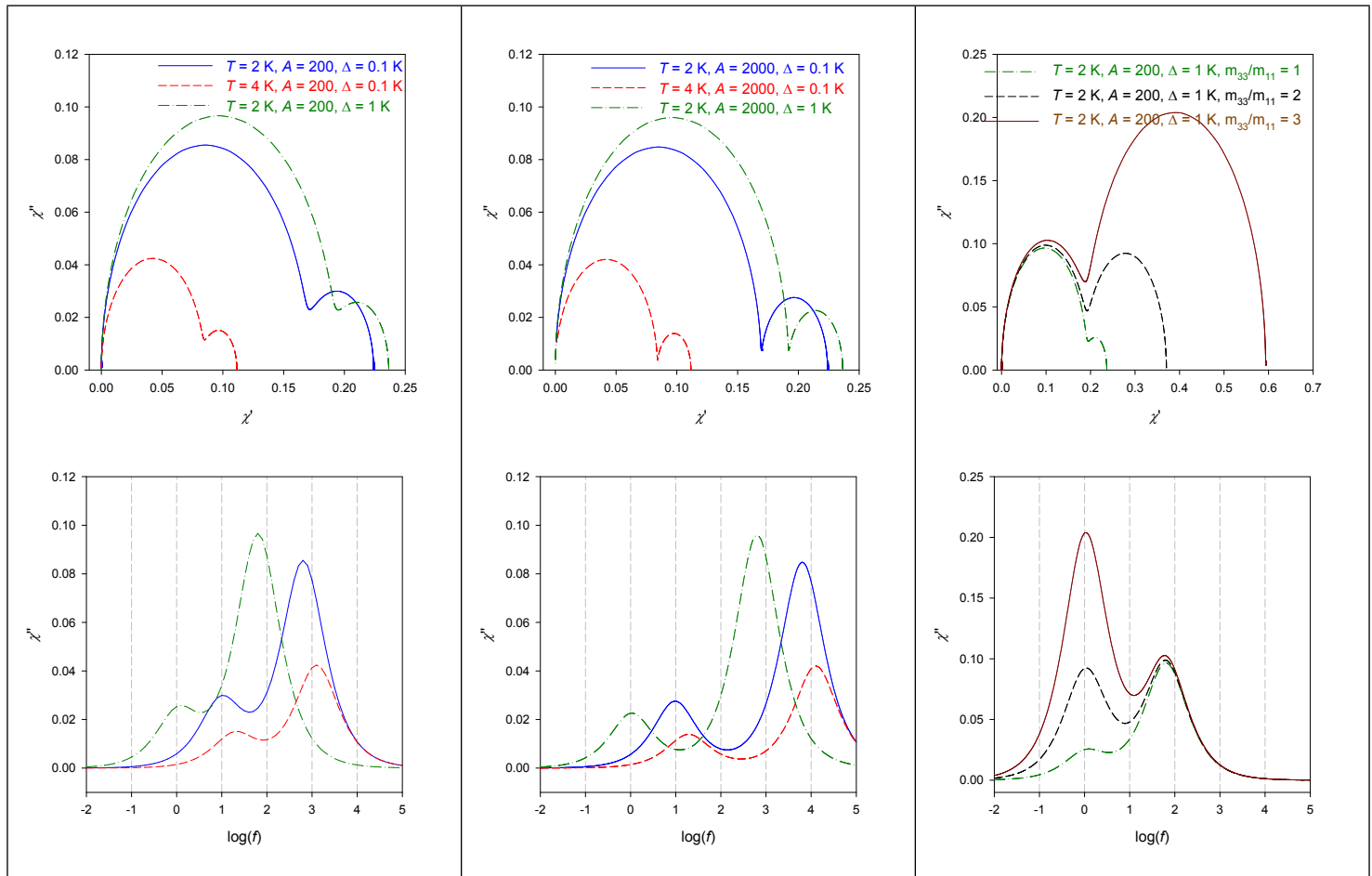


**Figure S9.** A modelling of the AC susceptibility behaviour using a three-level model of HO and CHIBOTARU.

- Since only the direct and Orbach processes are involved in such a modelling, the traditional Arrhenius-like plot cannot recover the observed acceleration of the relaxation time for the HF mode at the lowest temperatures supported by higher fields  $B_{\text{DC}} > 0.4 \text{ T}$ .
- The above model does not involve explicitly the effect of the magnetic field.
- Increase of the  $A$ -parameter causes a better separation of the peaks (HF peak is shifted to higher frequencies).
- Increase of the  $\Delta$ -parameter causes a reversed shift to lower frequencies.
- Increase of the  $m_{33}/m_{11}$  ratio causes an increase of the height of the LF peak.